



## Stability of liquid films covered by a carpet of self-propelled surfactant particles

Andrey Pototsky,<sup>1</sup> Uwe Thiele,<sup>2,\*</sup> and Holger Stark<sup>3,†</sup>

<sup>1</sup>*Department of Mathematics, Faculty of Science Engineering and Technology, Swinburne University of Technology, Hawthorn, Victoria 3122, Australia*

<sup>2</sup>*Institut für Theoretische Physik, Westfälische Wilhelms-Universität Münster, Wilhelm Klemm Straße 9, D-48149 Münster, Germany*

<sup>3</sup>*Institut für Theoretische Physik, Technische Universität Berlin, Hardenbergstrasse 36, 10623 Berlin, Germany*

(Received 28 July 2014; published 15 September 2014)

We consider a carpet of self-propelled particles at the liquid-gas interface of a liquid film on a solid substrate. The particles exert an excess pressure on the interface and also move along the interface while the swimming direction changes due to rotational diffusion. We study the intricate influence of these self-propelled insoluble surfactants on the stability of the film surface and show that depending on the strength of in-surface rotational diffusion and the absolute value of the in-surface swimming velocity, several characteristic instability modes can occur. In particular, rotational diffusion can either stabilize the film or induce instabilities of different character.

DOI: [10.1103/PhysRevE.90.030401](https://doi.org/10.1103/PhysRevE.90.030401)

PACS number(s): 68.15.+e, 05.40.-a, 05.65.+b

The understanding of the physical principles of the motion of self-propelled particles in viscous fluids [1–6], either in the bulk or at interfaces, is of primary importance for an increasing number of applications in microfluidics and medicine [7–9]. A particularly interesting emerging application of such swimmers is biocoatings formed using a suspension of living cells that is deposited onto a solid substrate before the solvent is removed, e.g., by evaporation. This technique is used to fabricate bacterial carpets consisting of living bacteria with rotating flagella that are attached head down to a polymer layer [10]. The created homogeneous monolayer of living cells is seen as a prototype of a novel biomaterial with remarkable applications, e.g., as artificial skin, self-cleaning coating, or biosensors [11–15]. Beside applications in biotechnology, free liquid-gas interfaces loaded with motile bacteria occur naturally, for example, at the sea surface [16]. Microswimmers at the interface of a thin liquid film also show interesting collective phenomena since even in a dilute suspension they interact with each other through the surface flow field initiated by gradients in the surface tension and curvatures in the height profile. In the following, we present an analysis of the stability of such thin films and demonstrate the subtle influence of in-plane swimming velocity and rotational diffusivity.

The proximity of swimmers to the liquid-gas interface inevitably modifies the local surface tension, which depends on the swimmer concentration similar to passive surfactant molecules and (nano)particles [17–20]. A gradient in the surface tension due to a nonuniform concentration generates fluid flow at the surface (solutocapillary Marangoni effect), a phenomenon well studied for passive surfactants. The impact of self-propelled surfactants, i.e., surfactants that are capable of moving autonomously, on the dynamics of liquid-gas interfaces (free surfaces), has been studied only in one special case. Namely, Ref. [21] investigates a monolayer of insoluble swimmers that are adsorbed at the free surface of a liquid film and exclusively swim into the direction perpendicular to the surface. That is, they are “head up” at all times and their motion along the liquid-gas interface is as for passive particles. As a

result, the swimmers generate an excess normal pressure and fluctuations in their density may “bulge” the interface locally. The induced fluid flow moves additional swimmers towards the bulge and increases the local excess pressure further. The interface becomes unstable if the combined stabilizing effect of translational diffusion and Marangoni flow towards regions of smaller swimmer concentration is too weak [21].

Here we show that self-propelled motion of the swimmer parallel to the liquid-gas interface (in-plane motion) together with rotational diffusion has a profound and nontrivial effect on the stability of the film. Depending on the strength of rotational diffusion and swimming velocity, the in-plane motion can stabilize a flat film or induce film instabilities of different character.

Consider a liquid film on a smooth homogeneous solid substrate with free liquid-gas interface as shown in Fig. 1(a). The liquid-gas interface is loaded with self-propelled particles, each characterized by a unit vector  $\mathbf{p}$  that gives the instantaneous direction of swimming with swimming velocity  $v_0$ . For mean film thicknesses below several hundred micrometers, the deformations of the liquid-gas interface are long-wave and can be described in the long-wave or lubrication approximation [22]. The position of a particle moving along the liquid-gas interface is given by the three-dimensional (3d) vector  $[\mathbf{r}(t), h(x, y, t)]$ , where  $\mathbf{r}(t) = [x(t), y(t)]$  is a two-dimensional (2d) position vector and  $h(x, y, t)$  is the local film height. In the long-wave approximation, the projections of the orientation vector  $\mathbf{p}$  orthogonal and parallel to the liquid-gas interface are approximated by its  $z$  component,  $p_\perp \approx p_z$ , and by  $\mathbf{p}_\parallel \approx (p_x, p_y)$ , respectively. Thus, the overdamped equations of motion for the  $i$ th particle become

$$\begin{aligned} \dot{\mathbf{r}}_i &= v_0(\mathbf{p}_\parallel)_i + \mathbf{U}_i + \boldsymbol{\chi}_i(t), \\ \dot{\mathbf{p}}_i &= [\boldsymbol{\eta}_i + \frac{1}{2}\boldsymbol{\Omega}_i] \times \mathbf{p}_i, \end{aligned} \quad (1)$$

where  $\boldsymbol{\chi}_i(t)$  with  $\langle \boldsymbol{\chi}_i(t) \otimes \boldsymbol{\chi}_k(t') \rangle = 2Mk_B T \delta_{ik} \delta(t - t') \mathbf{1}$  and  $\boldsymbol{\eta}_i$  with  $\langle \boldsymbol{\eta}_i(t) \otimes \boldsymbol{\eta}_k(t') \rangle = 2D_r \delta_{ik} \delta(t - t') \mathbf{1}_3$  represent translational (2d) and rotational (3d) noise, respectively [23]. They both influence the dynamics of the self-propelled surfactants at the liquid-gas interface.  $M$  is the translational mobility and  $D_r$  the rotational diffusivity of the swimmers (see note [24]),  $\mathbf{U}_i = [U_x(x_i, y_i), U_y(x_i, y_i)]$  is the surface velocity of the fluid,

\*u.thiele@uni-muenster.de; <http://www.uwethiele.de>

†holger.stark@tu-berlin.de

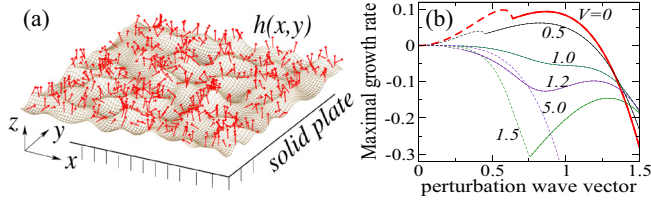


FIG. 1. (Color online) (a) Liquid-gas interface of a liquid film, loaded with self-propelled surfactant particles. Their swimming orientations are indicated by the unit vectors  $\mathbf{p}$ , shown by red arrows. (b) Influence of the in-line motion of self-propelled particles on film stability. Largest growth rate of a perturbation around a flat film plotted versus wave number for different values of the in-plane self-propulsion velocity  $V$  as indicated. Other parameters are  $D = 1$  and  $d = 0$ . Solid (dashed) lines correspond to oscillatory (steady) dynamics.

and  $\boldsymbol{\Omega}_i = \nabla \times \mathbf{U}_i = \Omega_i \mathbf{e}_z$  with  $\Omega = \partial_x U_y - \partial_y U_x$  denotes the vorticity at point  $(x_i, y_i)$ . For  $\boldsymbol{\xi}_i = \boldsymbol{\eta}_i = 0$ , Eqs. (1) reduce to the case studied in Ref. [25], where a swimmer moves in a prescribed time-independent Poiseuille flow field  $\mathbf{U}$ . In our case, the flow field is caused by variations in the liquid-film height and by the Marangoni effect.

So far, Eqs. (1) describe the dynamics of the full orientation vector  $\mathbf{p}$  at the interface. To reduce the dimensionality of the problem, we proceed to decouple the dynamics of its in-plane component  $\mathbf{p}_\parallel$  from the dynamics of the vertical orientation  $p_\perp$ . In spherical coordinates, we have  $p_\perp \approx p_z = \cos \theta$  and  $\mathbf{p}_\parallel \approx (p_x, p_y) = \sin \theta \mathbf{q}$  with  $\mathbf{q} = (\cos \phi, \sin \phi)$ . Assuming that the characteristic rotational diffusion time of the swimmers  $\tau \sim D_r^{-1}$  is much smaller than the characteristic relaxation time of the film thickness fluctuations (a plausible assumption for the quasistationary lubrication approximation), one may safely assume that the distribution of the vertical orientation of swimmers  $p_z$  adjusts “instantaneously” to some stationary distribution  $P(p_z)$ . This allows us to average Eqs. (1) over the angle  $\theta$  to obtain

$$\dot{\mathbf{r}}_i = v \mathbf{q}_i + \mathbf{U}_i + \boldsymbol{\chi}_i(t), \quad \dot{\phi}_i = \frac{1}{2} |\boldsymbol{\Omega}_i| + \xi_i(t), \quad (2)$$

where  $v = v_0 \langle \sqrt{1 - p_z^2} \rangle$ , with  $\langle \sqrt{1 - p_z^2} \rangle = \int \sqrt{1 - p_z^2} P(p_z) dp_z$  representing the average absolute value of  $\mathbf{p}_\parallel$ , and  $\xi(t)$  is a Gaussian white noise with  $\langle \xi_i(t) \xi_k(t') \rangle = 2D_r \delta_{ik} \delta(t - t')$ . Note that Eqs. (2) describe the 2d dynamics of a self-propelled particle with propulsion speed  $v$  moving in a fluid with velocity field  $\mathbf{U} = (U_x, U_y)$ .

The Smoluchowski equation for the surface particle density  $\rho(\mathbf{r}, \phi, t)$  corresponding to Eqs. (2) is a continuity equation with translational  $\mathbf{J}_t$  and rotational  $J_r$  currents that, as usual, contain drift and diffusional contributions (see, e.g., [26]):

$$\frac{\partial \rho}{\partial t} + \nabla \cdot \mathbf{J}_t + \frac{\partial J_r}{\partial \phi} = 0, \quad (3)$$

with  $\mathbf{J}_t = v \rho \mathbf{q} + \mathbf{U} \rho - M k_B T \nabla \rho$  and  $J_r = \Omega \rho / 2 - D_r \partial \rho / \partial \phi$ . Here,  $\nabla$  and  $\Delta$  denote, respectively, the nabla and Laplace operator in positional coordinates. Equation (3) is coupled to the thin-film equation via the solutocapillary Marangoni effect. Following Refs. [21,22], the equation for

the local film thickness  $h(x, y, t)$  is given by

$$\frac{\partial h}{\partial t} + \nabla \cdot \left( \frac{h^3}{3\mu} \nabla [\Sigma_0 \Delta h + \alpha \langle \rho \rangle] \right) + \nabla \cdot \left( \frac{h^2}{2\mu} \nabla \Sigma \right) = 0, \quad (4)$$

where  $\mu$  is the dynamic viscosity,  $\Sigma(x, y, t)$  is the concentration-dependent surface tension,  $\Sigma_0$  is the constant reference surface tension without surfactants (see note [27]), and  $\alpha \langle \rho \rangle$  describes the additional pressure exerted by the swimming particles onto the liquid-gas interface as in Ref. [21]. Here,  $\langle \rho \rangle(x, y, t) = \int_0^{2\pi} \rho(x, y, \phi, t) d\phi$  denotes the local particle density averaged over all swimming directions and  $\alpha = \langle p_z \rangle v_0 / M$  with  $\langle p_z \rangle = \int P(p_z) p_z dp_z$  is the negative of the force the interface exerts on the swimming particles in order to stop them in vertical direction [28]. Finally, the fluid velocity field at the free surface reads [22]

$$\mathbf{U} = \frac{h}{\mu} \nabla \Sigma + \frac{h^2}{2\mu} \nabla (\Sigma_0 \Delta h + \alpha \langle \rho \rangle). \quad (5)$$

To close our set of equations, we link surface tension  $\Sigma$  to particle density  $\rho$ . As any passive surfactant, self-propelled particles at the interface modify the local surface tension  $\Sigma$ . Here, we assume that the concentration is low; i.e., the surfactant particles are in a 2d gaseous state implying that  $\Sigma$  depends linearly on the local particle concentration  $\langle \rho \rangle$  (cf. Ref. [19]):

$$\Sigma = \Sigma_0 - \Gamma \langle \rho \rangle. \quad (6)$$

Typically,  $\Gamma > 0$ ; i.e., the surface tension decreases with increasing  $\langle \rho \rangle$  and the Marangoni flow is directed towards lower particle concentration.

Equations (3) to (6) form a closed system of nonlinear integro-differential equations for the two scalar fields  $h(x, y, t)$  and  $\rho(x, y, \phi, t)$ . It is important to note that for  $v = 0$  and  $\alpha = 0$ , the density is independent of the angle  $\phi$ , i.e.,  $\rho = \rho(x, y, t)$ , and Eqs. (3) to (6) reduce to the two usual coupled equations for film height  $h(x, y, t)$  and surfactant concentration  $\rho(x, y, t)$  for passive insoluble surfactant [22,29].

To nondimensionalize, we use  $h_0$  and  $h_0 \sqrt{\Sigma_0 / \Gamma \rho_0}$  as the vertical and horizontal length scale, respectively,  $\mu h_0 \Sigma_0 / (\Gamma^2 \rho_0^2)$  as the time scale, and the direction-averaged density of swimmers in the homogeneous state  $\langle \rho \rangle_0 = \int_0^{2\pi} \rho_0 / (2\pi) d\phi = \rho_0$  as the density scale. We introduce the dimensionless in-plane self-propulsion velocity  $V = v \mu \Sigma_0^{1/2} / (\Gamma \rho_0)^{3/2}$ , rotational diffusivity  $D = D_r h_0 \mu \Sigma_0 / (\Gamma \rho_0)^2$  [30], surface diffusivity  $d = k_B T M \mu / (h_0 \rho_0 \Gamma)$ , and excess pressure  $\beta = \alpha h_0 / \Gamma$ . The dimensionless equations of motion derived from Eqs. (3), (4), and (5) are summarized in the Supplemental Material [31].

The trivial homogeneous stationary state corresponds to a flat film covered uniformly by particles, i.e.,  $\rho = 1/(2\pi)$  and  $h = 1$ . Any small-amplitude perturbation of the trivial uniform state can be represented as

$$\delta h(\mathbf{r}, t) = \int \hat{h}(\mathbf{k}) e^{\gamma(\mathbf{k})t} e^{i\mathbf{k}\mathbf{r}} d\mathbf{k}, \quad (7)$$

$$\delta \rho(\mathbf{r}, \phi, t) = \lim_{N \rightarrow \infty} \frac{1}{2\pi} \sum_{n=-N}^N e^{In\phi} \int W_n(\mathbf{k}) e^{\gamma(\mathbf{k})t} e^{i\mathbf{k}\mathbf{r}} d\mathbf{k},$$

with small amplitudes  $\hat{h}(\mathbf{k})$  and  $W_n(\mathbf{k})$ , the wave vector  $\mathbf{k} = (k_x, k_y)$ , and the growth rate  $\gamma(\mathbf{k})$ . For any fixed number  $N$  of the Fourier modes, the growth rate  $\gamma(\mathbf{k})$  of the fastest growing perturbation is found by solving the eigenvalue problem obtained by linearizing the dimensionless Eqs. (3), (4), and (5) [31]. For the parameter values used here, the results have converged for  $N = 10$ .

In what follows, we set  $d = 0$  and focus on the most striking effects of the in-plane motion and in-plane rotational diffusion of the swimmers on film stability. The choice of  $d = 0$  is motivated by estimating the ratio  $V^2/(Dd) = v^2/(D_r M k_B T) \gg 1$  using thermal values for both diffusion coefficients with  $R = 1 \mu\text{m}$  and  $v = 1 \mu\text{m/s}$ . As the eigenvalues  $\gamma(\mathbf{k})$  only depend on the absolute value of  $\mathbf{k}$  but not on its direction (spatial isotropy), we compute the growth rate  $\text{Re}(\gamma)$  as a function of  $k$ .

As a reference we set the excess pressure parameter  $\beta = 3$  to be above the critical value of  $\beta_c = 2$ , where the long-wave steady instability sets in for  $V = 0$ . This case corresponds to particles that only swim perpendicularly to the free surface as studied in Ref. [21]. The corresponding dispersion relation  $\text{Re}(\gamma)$  vs  $k$  is plotted as a heavy solid line in Fig. 1(b) and indicates that the excess pressure due to the upwards swimming surfactants drives the film unstable. Figure 1(b) also shows how the film is stabilized by the in-plane self-propelled particle motion, i.e., when increasing  $V$  from zero (here, at fixed rotational diffusion  $D = 1$ ). We understand this stabilization qualitatively since active motion along the interface acts like the stabilizing translational diffusion with an effective diffusivity  $d_{\text{eff}} = V^2/2D$  on time scales larger than the orientational correlation time  $D^{-1}$  [32–34]. We further note that at low  $V$  the dispersion relation has two maxima that correspond to a steady (growing drops and holes) and an oscillatory instability (traveling waves) mode that dominate at  $V = 0$  and  $V = 0.5$ , respectively. The onset of the steady instability occurs at  $V \approx 1$  at zero wave number.

The accompanying stability diagram in the  $(V, d_{\text{eff}})$ -parameter plane [Fig. 2(a)] provides quantitative insight into the stabilization of the liquid film. It reveals an intermediate range of  $d_{\text{eff}} = V^2/2D$  where the film is stable. A small effective diffusivity  $d_{\text{eff}}$  (large  $D$ ) cannot stabilize the film. The film becomes stable when  $d_{\text{eff}}$  exceeds a threshold value, which exactly agrees with the stabilizing translational diffusivity obtained in Ref. [21] for swimmers with purely head-up orientation (red dashed line). Indeed, by expanding the full density  $\rho(x, y, \phi, t)$  into angular moments and deriving dynamic equations for the moments from Eq. (3), one can formulate a Smoluchowski equation for  $\langle \rho \rangle(x, y, t) = \int_0^{2\pi} \rho(x, y, \phi, t) d\phi$  on time scales larger than  $D^{-1}$  and on large length scales, where the active motion only contributes to an effective translational diffusion constant  $d + d_{\text{eff}}$  [35,36]. So, one obtains the density equation employed in Ref. [29] for passive surfactants and in Ref. [21] for swimmers with purely head-up orientation.

The selected dispersion relations for the growth rate in Figs. 2(b) and 2(c) at  $V = 1$  reveal a small wavelength instability for  $D \approx 0$  (curve 1) to  $D \approx 0.6$ , which corresponds to the unstable region in (a) for large  $d_{\text{eff}}$ . A stability analysis of our dynamic equations for  $D = 0$  at a fixed delta-peaked distribution of the swimming direction reveals a growing

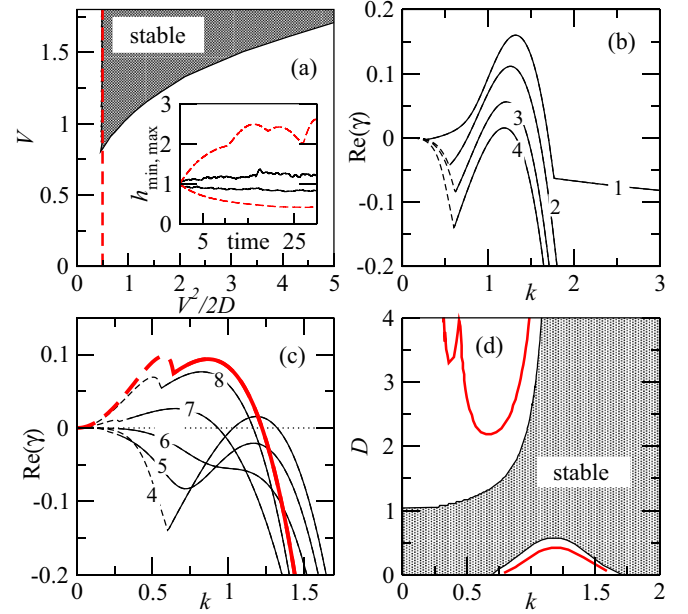


FIG. 2. (Color online) (a) Stability diagram in the plane  $(d_{\text{eff}} = V^2/2D, V)$  at fixed  $\beta = 3$  and  $d = 0$ . The inset shows the time evolution of the minimum and maximum of the local film thickness in the smooth particle dynamics simulations for  $V = 0$  (dashed lines) and  $V = 5$  (solid lines) at  $D = 1$ . (b) and (c) The dispersion relations (maximal  $\text{Re}[\gamma(k)]$ ) for  $V = 1$  and different  $D$  as indicated by numbers near each curve: 1,  $D = 0.001$ ; 2,  $D = 0.1$ ; 3,  $D = 0.3$ ; 4,  $D = 0.5$ ; 5,  $D = 0.7$ ; 6,  $D = 1$ ; 7,  $D = 2$ ; and 8,  $D = 10$ . Solid (dashed) lines correspond to oscillatory (steady) perturbations. The heavy solid line represents  $D \rightarrow \infty$  and coincides with the curve for  $V = 0$  in Fig. 1(b). (d) Stability diagram in the plane  $(D, k)$ . The solid line represents the level line of the dispersion relation at  $\text{Re}(\gamma) = 0.03$  to illustrate its bimodal character.

density and height modulation wave that travels with the swimming speed  $V$ . This implies that dense swimmer regions do not disperse and render the film unstable. With increasing  $D$  the swimming direction starts to diffuse which suppresses the traveling waves more and more (depending on  $k$ ) until at  $D \approx 0.6$  the trivial state is stable. The stability diagram in the  $(k, D)$  plane in Fig. 2(d) illustrates the qualitatively different character of the instabilities at low and large  $D$ . Above the stable range at intermediate  $D$ , the film becomes again unstable when the effective translational diffusivity  $V^2/2D$  becomes too small. The onset occurs at  $k = 0$  as a steady instability; however, with further increasing  $D$  the dispersion relation develops a bimodal character as indicated in Fig. 2(d) by the shown level line. Note, finally, that at large  $D$  [ $V^2/D \rightarrow 0$ ], the dispersion relation is identical to the one in the unstable reference case of purely perpendicular swimming [red curve in Fig. 2(c)].

In order to confirm the predicted stabilization of a liquid film by motile surfactant particles, we numerically solve the thin-film equation [Eq. (4)] in a  $L \times L$  square box with periodic boundary conditions, coupled to the equations of motion [Eqs. (2)] for  $n = 500$  individual point swimmers. Their discrete spatial distribution is translated into a smooth particle density function  $\rho(x, y, t)$  employing the method of

smooth particle dynamics [37], as outlined in the Supplemental Material [31].

Fixing the remaining parameters as in Fig. 1(b), we vary the self-propulsion velocity  $V$ . From the linear stability analysis we expect that the flat film is linearly unstable for  $V = 0$  and linearly stable for  $V = 5$ . Starting from randomly located and oriented particles on the flat film surface, we observe a time evolution that is noisy in both cases due to the coupling of the continuum equation to the discrete particle dynamics. This can be appreciated in the inset of Fig. 2(a) showing the time evolution of the minimum and maximum of the local film thickness for  $V = 0$  (dashed lines) and  $V = 5$  (solid lines) [31].

One discerns a clear difference between the two cases: For  $V = 0$ , the swimmer-induced instability of the flat film is apparent. The amplitude of the surface deflections first grows before at later times it varies (in a potentially chaotic way) about a maximum that is by about a factor 2 larger than the mean film thickness  $h = 1$ . This resembles a regime of interacting nonlinear “traveling waves” as predicted in Ref. [21]. However, for swimmers with in-plane motility (here,  $V = 5$ ), one finds that after a small initial growth the deformation amplitude soon saturates and then fluctuates about a (small) finite amplitude that is by about a factor 2 smaller than  $h = 1$ . This indicates that the instability is strongly suppressed. The remaining fluctuations of the film surface are a consequence of the hybrid calculations where the discrete stochastic dynamics of the finite number of swimmers is coupled to the continuum model for the evolution of the film height.

In conclusion, we have shown that rotational diffusion can play a distinctive role in the motion of self-propelled surfactants on liquid films. Depending on its relative strength, it can stabilize or destabilize the film and may also change the

qualitative character of the instability and, in consequence, the nonlinear behavior. More specifically, our analysis shows the flat film can be destabilized according to two different scenarios: (i) through the steady long-wave instability at  $V^2/2D = 0.5$  and (ii) through the oscillatory finite-wavelength instability along the solid line in Fig. 2(a).

However, one needs to show that such a system is experimentally feasible as was done for the “head-up” self-propelled particles in Ref. [21]. Next we assess whether this also applies for the stabilization of the film due to the combined action of the rotational diffusivity  $D$  and the in-plane velocity  $V$ , reported here. As an example, we estimate the dimensionless  $V$  and  $D$  for self-propelled Janus particles [38] in a water film at room temperature: thus we take  $\mu = 10^{-3} \text{ kg m}^{-1} \text{ s}^{-1}$ ,  $\Sigma_0 = 10^{-1} \text{ N m}^{-1}$ ,  $\Gamma = 10^3 \text{ kg m}^2 \text{ s}^{-2} \text{ mol}^{-1}$  (from [21]),  $v = 10^{-6} \text{ m s}^{-1}$ ,  $R = 10^{-6} \text{ m}$  (from [38]). In addition, we estimate the (largest possible) average density  $\rho_0 \approx (\pi R^2)^{-1} \approx 10^{-12} \text{ mol m}^{-2}$  and take  $h_0 = 10^{-4} \text{ m}$ . Taking into account that for a spherical Brownian particle  $D_r = 3k_B T M / 4R^2$  and  $M = (6\pi\mu R)^{-1}$  we obtain  $V \sim 10^4$  and  $V^2/D \sim 10^{-1}$ . These estimates show that self-propelled Janus particles in a  $100 \mu\text{m}$  thick water film approximately fall onto the vertical dashed line in Fig. 2(a). Consequently, by fine tuning the radius  $R$  of the particles ( $V \propto R^3$  and  $V^2/D \propto R^5$  at largest possible density) or the self-propulsion velocity  $v$ , one can induce or suppress the long-wave steady instability of the film.

A.P. thanks the research training group GRK 1558 funded by Deutsche Forschungsgemeinschaft (DFG) for financial support. The authors are grateful to the Newton Institute in Cambridge, UK, for its hospitality during a common stay at the program “Mathematical Modelling and Analysis of Complex Fluids and Active Media in Evolving Domains”.

- 
- [1] E. Lauga and T. R. Powers, *Rep. Prog. Phys.* **72**, 096601 (2009).  
 [2] D. Saintillan and M. J. Shelley, *C. R. Phys.* **14**, 497 (2013).  
 [3] I. S. Aranson, *C. R. Phys.* **14**, 518 (2013).  
 [4] R. Kapral, *J. Chem. Phys.* **138**, 020901 (2013).  
 [5] A. Zöttl and H. Stark, *Phys. Rev. Lett.* **112**, 118101 (2014).  
 [6] M. Hennes, K. Wolff, and H. Stark, *Phys. Rev. Lett.* **112**, 238104 (2014).  
 [7] S. K. Chang, V. N. Paunov, D. N. Petsev, and O. D. Velev, *Nat. Mater.* **6**, 235 (2007).  
 [8] M. S. Baker, V. Yadav, S. Ayusman, and S. T. Phillips, *Angew. Chem. Int. Ed.* **52**, 10295 (2013).  
 [9] J. D. Yadav, V. Freedman, M. Grinstaff, and S. Ayusman, *Angew. Chem. Int. Ed.* **52**, 10997 (2013).  
 [10] N. Darnton, L. Turner, K. Breuer, and H. C. Berg, *Biophys. J.* **86**, 1863 (2004).  
 [11] K. Efimenko, J. Finlay, M. E. Callow, J. A. Callow, and J. Genzer, *ACS Appl. Mater. Interfaces* **1**, 1031 (2009).  
 [12] Q. Xu, C. Barrios, T. Cutright, and B. Newby, *Environ. Sci. Pollut. Res.* **12**, 278 (2005).  
 [13] R. F. Bennett, *Case Study of an Environmental Contaminant* (Cambridge University Press, Cambridge, 1996), p. 21.  
 [14] K. D. Weiss, *Prog. Polym. Sci.* **22**, 203 (1997).  
 [15] M. Fidaleo, S. Charaniya, C. Solheid, U. Diel, M. Laudon, H. Ge, L. E. Scriven, and M. C. Flickinger, *Biotechnol. Bioeng.* **95**, 446 (2006).  
 [16] M. I. Gladushev, *Biophysics of the Surface Microlayer of Aquatic Ecosystems* (IWA Publishing, London, 2002).  
 [17] M. J. Rosen and J. T. Kunjappu, *Surfactants and Interfacial Phenomena* (John Wiley & Sons, Hoboken, NJ, 2012).  
 [18] B. Binks, *Curr. Opin. Colloid Interface Sci.* **7**, 21 (2002).  
 [19] U. Thiele, A. J. Archer, and M. Plapp, *Phys. Fluids* **24**, 102107 (2012).  
 [20] V. Garbin, J. C. Crocker, and K. J. Stebe, *Langmuir* **28**, 1663 (2012).  
 [21] S. Alonso and A. S. Mikhailov, *Phys. Rev. E* **79**, 061906 (2009).  
 [22] A. Oron, S. Davis, and S. Bankoff, *Rev. Mod. Phys.* **69**, 931 (1997).  
 [23] Here  $\otimes$  stands for the tensor product between two vectors,  $\mathbf{1}$  is the unit  $2 \times 2$  matrix, and  $\mathbf{1}_3$  is the unit  $3 \times 3$  matrix.  
 [24] The translational noise is assumed to be purely thermal, while the rotational noise can be decomposed into the thermal part and the kinetic part that corresponds to the frequent tumbling events in case of the run-and-tumble particles (cf. [26]).  
 [25] A. Zöttl and H. Stark, *Phys. Rev. Lett.* **108**, 218104 (2012).

- [26] A. Pototsky and H. Stark, *Europhys. Lett.* **98**, 50004 (2012).
- [27] The capillary pressure term  $\Sigma_0 \Delta h$  is a direct consequence of the long-wave approximation [22]. However, to recover the gradient dynamics structure discussed in Ref. [19] from Eqs. (3) and (4) in the “passive” limit  $v, \alpha \rightarrow 0$ , the term  $\nabla \cdot (\Sigma \nabla h)$  would be used. The difference between the two forms is negligible as it is only  $O(\varepsilon^2)$ , where  $\varepsilon$  is the smallness parameter of the long-wave approximation.
- [28] Note that  $\alpha$  depends on the mobility of the particle  $M$ , which in its turn is linked to the particle radius via the Stokes law, i.e.,  $M = (6\pi\mu R)^{-1}$  for spherical particles of radius  $R$ .
- [29] L. W. Schwartz, D. E. Weidner, and R. R. Eley, *Langmuir* **11**, 3690 (1995).
- [30] Note that for the dimensionless thermal rotational diffusion  $D = k_B T \sigma_0 / (8\pi \Gamma^2 \rho_0^2) \times h_0 / R^3$ , where  $R$  is the radius of the spherical swimmer.
- [31] See Supplemental Material at <http://link.aps.org/supplemental/10.1103/PhysRevE.90.030401> for details of the linear stability analysis and two video files showing the temporal evolution of the system.
- [32] J. R. Howse, R. A. L. Jones, A. J. Ryan, T. Gough, R. Vafabakhsh, and R. Golestanian, *Phys. Rev. Lett.* **99**, 048102 (2007).
- [33] J. Palacci, C. Cottin-Bizonne, C. Ybert, and L. Bocquet, *Phys. Rev. Lett.* **105**, 088304 (2010).
- [34] M. Enculescu and H. Stark, *Phys. Rev. Lett.* **107**, 058301 (2011).
- [35] R. Golestanian, *Phys. Rev. Lett.* **108**, 038303 (2012).
- [36] O. Pohl and H. Stark, *Phys. Rev. Lett.* **112**, 238303 (2014).
- [37] W. G. Hoover, *Smooth Particle Applied Mechanics: The State of the Art*, Advanced Series in Nonlinear Dynamics Vol. 25 (World Scientific Publishing Co. Pte. Ltd., Singapore, 2006).
- [38] I. Buttinoni, F. Kümmel, G. Volpe, and C. Bechinger, *J. Phys.: Condens. Matter* **24**, 284129 (2012).